

The Order of Accuracy Related to the Error from Source Approximation in the Method of Characteristics for Purely Absorbing Materials in Planar Geometry

Authors: Ji-Pu Wang, Zhen-Wen Wei, Can Huang, William Martin, Brendan Kochunas, Qi-Cang Shen, Si-Juan Chen, Martin Pilch, Qi-Cang Shen, Si-Juan Chen


Date: 2026-02-12T22:09:40+00:00

Abstract

The method of characteristics (MoC) is a well-established tool for lattice physics calculations, offering advantages such as accurate representations of both lattice geometry and boundary conditions. The flat source (FS) approximation is the most commonly used approach, while the linear source (LS) approximation enhances accuracy by preserving higher-order spatial moments of the neutron source. However, determining the order of accuracy (OoA) for spatial discretization in MoC is challenging, particularly for the LS approximation. This complexity arises because MoC employs two spatial meshes: the fission source region (FSR) mesh and a set of characteristic rays used to integrate the transport equation over the FSR mesh. In this study, we analyze the spatial order of accuracy of MoC in planar geometry for both FS and LS approximations in relation to the distributed source. Our theoretical predictions are consistent with the numerical results using the Method of Manufactured Solutions (MMS). The results demonstrate that the FS approximation achieves second-order accuracy, while the LS approximation attains fourth-order accuracy.

Full Text

Preamble

The order of accuracy related to the error from source approximation in the method of characteristics for purely absorbing materials in planar geometry*
Ji-Pu Wang,¹ Zhen-Wen Wei ,¹ Can Huang,¹ William Martin,² Brendan Kochunas,² Qi-Cang Shen,³, [†] Si-Juan Chen,¹, [‡] and Martin Pilch⁴ ¹Shenzhen Key Laboratory of Nuclear and Radiation Safety, Institute for Advanced Study

in Nuclear Energy & Safety, College of Physics and Optoelectronic Engineering, Shenzhen University, Shenzhen 518060, China ²Department of Nuclear Engineering and Radiological Sciences, University of Michigan, Ann Arbor, MI 48109, USA ³Institute of Applied Physics and Computational Mathematics (IAPCM),

6 Huayuan Road, Haidian District, Beijing, 100088, China

4MPilchConsulting, 26 Mustang Mesa Trail, Tijeras, NM 87059, USA The method of characteristics (MoC) is a well-established tool for lattice physics calculations, offering advantages such as accurate representation of both lattice geometry and boundary conditions. The flat source (FS) approximation is the most commonly used approach, whereas the linear source (LS) approximation enhances the accuracy by preserving the higher-order spatial moments of the neutron source. However, determining the order of accuracy (OoA) for spatial discretization in the MoC is challenging, particularly for the LS approximation. This complexity arises because MoC employs two spatial meshes: the fission source region (FSR) mesh and a set of characteristic rays used to integrate the transport equation over the FSR mesh. In this study, we analyzed the spatial order of accuracy of the MoC in planar geometry for both FS and LS approximations in relation to the distributed source. Our theoretical predictions are consistent with the numerical results obtained using the Method of Manufactured Solutions (MMS). The results demonstrate that the FS approximation achieves second-order accuracy, whereas the LS approximation attains fourth-order accuracy.

Keywords: Method of characteristics, Order of accuracy, Flat source approximation, Linear source approximation, Method of manufactured solutions

INTRODUCTION

The method of characteristics (MoC) is a well-established tool for lattice-physics calculations. More recently, it has been observed in such state-of-the-art deterministic high-fidelity reactor physics codes as MPACT [1], OpenMOC [2], NECP-X [3], and Proteus-MOC [4], offering advantages such as high parallel efficiency and accurate representations of both complex geometry and boundary conditions [5]. The flat source (FS) approximation is the most commonly used approach [6-8], whereas the linear source (LS) approximation is employed when higher accuracy is required [9, 10]. * This work was supported by the Stable Support Plan Program under Shenzhen Natural Science Fund Contract (No. 20220811012323001), the LingChuang Research Project of China National Nuclear Corporation under Contract (No. CNNC-LCKY-202266), the Shenzhen Key Laboratory of Nuclear and Radiation Safety of Shenzhen Science and Technology Innovation Commission under Contract (No. ZDSYS20230626091501002), the Pengcheng Peacock Plan Distinguished Talent project (No.827-000712), the Shenzhen Science and Technology Innovation Commission Key Technical Project under Contract

(No.s JSGG20220831110607013 and KJZD20231023100200001), the Young Innovative Talent in Guangdong Province No. 2023KQNCX065, the Teaching Reform Research Programs under Shenzhen University Contract (Nos. JG000066010107, JG000033090185, and JG2022072), and the Teaching Reform Research Program under Guangdong Provincial Department of Education Contract JG2024085). This work was also supported by the Consortium for Advanced Simulation of Light Water Reactors (<https://casl.gov/>), an Energy Innovation Hub (<http://www.energy.gov/hubs>) for Modeling and Simulation of Nuclear Reactors, under the U.S. Department of Energy Contract (No. DE-AC05-00OR22725). † Corresponding author, shen_qicang@iapcm.ac.cn ‡ Corresponding author, chensijuan@szu.edu.cn While significant attention has been given to implementing these numerical methods in reactor physics codes and improving their performance, the verification of these codes has received limited research [11]. This study provides a more theoretical and rigorous demonstration. Verification is crucial to ensuring the correctness of both the numerical methods and their implementations. The Consortium for Advanced Simulation of Light Water Reactors (CASL) [12] has set a benchmark in this regard by dedicating substantial efforts to Verification and Validation (V&V) [13] to maintain high code quality and verified methodology. A critical aspect of this process involves analyzing discretization errors in complex methods such as the method of characteristics (MoC) within the MPACT code [14].

MoC utilizes a non-standard spatial discretization method that involves two sets of spatial meshes: the FSR mesh and a set of characteristic rays used to integrate the transport equation over the FSR mesh. The interaction between the characteristic rays and the FSR mesh complicates the error analysis of MoC solutions, making it difficult to determine the order of accuracy (OoA) of MoC's spatial discretization.

Our preliminary attempt to determine the OoA related to source approximation in one-dimensional (1D) geometry was presented at the M&C 2017 conference [15] and ICONE 30 [16], although they lacked a rigorous proof. In this study, we focused on purely absorbing materials and provided a formal proof of the OoA for spatial resolution in planar geometry for both FS and LS approximations. We verified our predictions using the Method of Manufactured Solutions (MMS) [17], which provides an analytical solution for comparison. The use of 1D geometry eliminates the complexity of ray spacing, allowing us to isolate and analyze the error convergence rate over the FSR mesh refinements.

Understanding the error convergence rate, or the order of accuracy, for both FS and LS approximations is valuable for assessing the errors introduced in the MoC and guiding the selection of the FSR mesh size. Furthermore, quantifying and locating errors can aid in the development of more accurate MoC schemes. Additionally, knowledge of the theoretical order of accuracy can be used to verify reactor physics codes through Code Verification methods such as MMS.

Section II presents the theoretical prediction of the order of accuracy, focusing on distributed sources. Unlike previous studies on spatial discretization [18,

[19], this study begins with the exact solution along the characteristic rays and quantitatively tracks the error propagation, making it easier to generalize the analysis from FS to LS approximations. Section III provides numerical results [20] that validate our theoretical predictions using the MMS and the Method of Exact Solutions (MES). We also verified the MoC code developed for this study by considering both polynomial and non-polynomial function forms. Additionally, we apply Ganapol's infinite cylinder case [21] using the production code MPACT [1] to confirm the order of accuracy. Section IV summarizes our conclusions, demonstrating that the FS approximation achieves second-order accuracy, while the LS approximation attains fourth-order accuracy.

In the MoC, the angular flux along a characteristic can be analytically integrated using an assumed form of the source term $q(x, \mu)$. $\partial\psi(x, \mu) + \Sigma_t\psi(x, \mu) = q(x, \mu)$ where μ is the direction cosine, x is the position, $\psi(x, \mu)$ is the angular neutron flux, and Σ_t is the macroscopic total cross-section.

For simplicity, we illustrate the theory in a one-dimensional geometry and apply the following assumptions: homogeneous materials, isotropic scattering, and energy independence. The coordinate of this planar model used in our theory is shown in Fig. 1 [Figure 1: see original paper].

Integrating the above equation over a canonical spatial cell j , where $x_{j-1/2} < x < x_{j+1/2}$, yields the neutron balance equation within this cell, which in turn can be used to derive the expression for the cell-averaged angular flux. To further simplify the algebra, the first cell is used to represent the canonical cell with $z' = 0$ corresponding to $x_{1/2}$ and $z' = z$ corresponding to $x_{3/2}$. Operating on Equation (1) with operation $\int_0^z (\cdot) dz'$ yields $\bar{\psi}(\mu) = \bar{q}(\mu) \psi(0, \mu) - \psi(z, \mu)$, where $\bar{\psi}(\mu) = \int_0^z \psi(z', \mu) dz'$, $\bar{q}(\mu) = \int_0^z q(z', \mu) dz'$.

The exiting angular flux with respect to this cell can also be solved analytically using an integration factor $e^{-\Sigma_t z}$. Substituting this result back into Eq. (1) provides an explicit solution for the angular flux, as follows: $\psi(z, \mu) = \psi(0, \mu) e^{-\Sigma_t z} + \int_0^z q(z', \mu) e^{-\Sigma_t(z-z')} dz'$. $\bar{\psi}(\mu) = \int_0^z \psi(z', \mu) dz' = \psi(0, \mu) \int_0^z e^{-\Sigma_t z'} dz' + \int_0^z \int_0^{z'} q(z'', \mu) e^{-\Sigma_t(z'-z'')} dz'' dz'$.

The approximating cell-averaged angular flux $\tilde{\bar{\psi}}$ is expressed below, where \tilde{q} approximates q and $\tilde{\bar{q}}$ is the average of the approximating source \tilde{q} . $\tilde{\bar{\psi}}(\mu) = \psi(0, \mu) \int_0^z e^{-\Sigma_t z'} dz' + \int_0^z \tilde{q}(z', \mu) dz'$ The error E is defined as the difference between the analytical expression of the cell-averaged angular flux $\bar{\psi}$ given in Eq. (5) and its approximation $\tilde{\bar{\psi}}$ presented in Eq. (6).

$E = \bar{\psi}(\mu) - \tilde{\bar{\psi}}(\mu) = \int_0^z q(z', \mu) e^{-\Sigma_t(z-z')} dz' - \int_0^z \tilde{q}(z', \mu) dz'$ II. FORMAL ORDER OF ACCURACY Inserting Eq. (4) into Eq. (2) yields Fig. 1. Global and local coordinate systems This error depends on how well $\tilde{q}(z', \mu)$ approximates the true source distribution. Equation (7) is evaluated for both FS and LS approximations and is the basis for the error analysis throughout the paper.

When different approximations (e.g., FS and LS approximations) are used, the following definition of $\tilde{q}(z')$ is taken, with angular dependence dropped to avoid symbolic entanglements, $\tilde{q}(z') = q_0 + q_1(z' - z_c)$ flat source linear source where z_c refers to the midpoint of local coordinate and we define the zeroth source moment as follows $\int q(z') dz'$, and the first source moment as follows $\int q(z')(z' - z_c) dz'$ (cid:20) 1 (cid:90) z (cid:104) $z'q(z') - z_cq(z')$ (cid:20) 1 (cid:105) $\int z'q(z') dz' - z_c \int q(z') dz'$ (cid:21) 12 Note that the definition of q_0 indicates that $\tilde{q} = \tilde{q} = q_0$.

In addition, note that the definition q_1 involves a transformation from a global coordinate system to a local one, which is briefly illustrated below.

Assume that source $Q(x)$ is the total source in a slab geometry in a global coordinate system $0 < x < x_{max}$. The (cid:1) is to be source $Q(x)$ over a canonical cell (cid:0) $x_{j-1/2}, x_{j+1/2}$ linearized as $q_0 + q_1 \cdot (z' - z_c)$, where z' is the local coordinate in the current cell j originated at the left edge of the cell, as shown in Fig. 2 [Figure 2: see original paper].

Next, we show how to obtain the first spatial source moment q_1 from the global quantities $Q(x)$.

$Q(x) \tilde{q}(z') = q_0 + q_1(z' - z_c) \cdot$ (cid:82) $\int_0 [\cdot] dz'$ on the above Eq. (11) Performing operation 1 gives $Q(x) = q_0$. (cid:82) $\int_0 [\cdot] (z' - z_c) dz'$ on Eq. (11). The Perform operation 1 right-hand-side (RHS) gives (cid:90) z RHS = (cid:8)(cid:2) $q_0 + q_1(z' - z_c)$ (cid:3) $(z' - z_c)$ (cid:9) $dz' = q_1 z^2$ Fig. 2. Global and local coordinate systems presented with assumed source distribution Therefore, the first spatial source moment can be expressed (cid:104) $Q(x) \cdot x - x_c \cdot Q(x)$ (cid:105) 12 Now, we consider the expression for a fixed source, consisting of both scattering and distributed source components, as follows: $q(z', \mu) =$ (cid:90) 1 $\psi(z', \mu) d\mu + q_{MMS}(z', \mu)$.

The left-hand side (LHS) gives LHS = (cid:90) z $[\tilde{q}(z')(z' - z_c)] dz'$ (cid:90) $x_{j+1/2} [Q(x)(x - x_c)] dx$ (cid:0) $x - x_{j-1/2}$ (cid:1) $x_{j-1/2}$ (cid:90) $x_{j+1/2}$ (cid:104) $Q(x) x - x_c Q(x)$ (cid:105) $[Q(x) x - Q(x) x_c] dx$ Both scattering and distributed components contribute to the total source term. The distributed source, labeled with the subscript MMS, represents a known mathematical source commonly used in Code Verification.

The scattering source depends on iterative updates from neutron interactions, which makes it difficult to include in the analytic error analysis. To keep the methodology clear, we consider only the distributed source in this study. With this simplification, the structure of the source can be expressed through its zeroth spatial source moment, the $q_{0,(n)}(\mu)$, and the first spatial source moment, the $q_{1,(n)}(\mu)$, defined in MMS (μ) ,

1. Constant Component

Eq. (17): $q_{0,(n)}(\mu) = M^{(n-1)} q_{1,(n)}(\mu) = q_{MMS}^{(n-1)}(z', \mu) dz' - z_{scat}^{(n-1)}(\mu) + q_{0}^{(n-1)}(z', \mu) - z_{cq}^{(n-1)}(z', \mu) - z_{c}^{(n-1)}(\mu) + q_{1}^{(n-1)}(z', \mu)$, where $\hat{\psi} = 1$ is the first spatial moment of $\hat{\psi}$ is its approximation, ω_m is the coefficient of Legendre-Gauss quadrature. The superscripts (n) and $(n-1)$ denote the iteration indices, and once the convergence criterion is achieved, these terms become equivalent, allowing the superscripts to be omitted.

Since linear systems obey the superposition principle, the total order of accuracy depends on the worst-case approximation between the distributed and scattering sources. This study focuses on the order of accuracy of the distributed source, assuming the scattering source is zero, which is valid for purely absorbing materials.

When the average of the approximated distributed source $\tilde{q}(z')$ exactly equals the average of the true source $q(z')$, the first two terms in the error defined in Eq. (7) cancel out, reducing the error to a simplified form:

$E = -e^{-\Sigma t} \int_0^z q(z', \mu) dz' - \tilde{q}(z', \mu) dz'$ Next, we analyze the error behavior for FS and LS approximations separately.

A. Flat Source (FS) Approximation FS approximation implies the following $\tilde{q}(z') = q_0$.

Using Eq. (18) to evaluate the error introduced into the cell-averaged angular flux due to FS approximation $E = -e^{-\Sigma t} \int_0^z q(z', \mu) dz' - q_0 \int_0^z dz'$ To begin with, three low-order monomial cases were examined: constant, linear, and quadratic source distributions.

Based on these cases, the general polynomial case can be realized by superposition. Conversely, these low-order cases can be viewed as components of a more general source.

For a constant source distribution, $q(z') = c$, $0 < z' < z$, the associated error is $E = 0$. This result was verified using our MoC 1D code, which demonstrated that the solution maintained machine precision accuracy, irrespective of the grid resolution. This outcome is expected, as q_0 precisely represents a constant source. Consequently, the flat source approximation introduced no error. This can be easily proven as follows:

$E = -e^{-\Sigma t} \int_0^z c dz' - c \int_0^z dz' = 0$.

2. Linear Component

If the source is linear in space, the FS approximation introduces an error of second order with the mesh size. Assuming $q(z') = z'$, $0 < z' < z$, the error

can be evaluated using Eq. (20). Finally, it is expanded to a Taylor series to obtain the order of accuracy (OoA).

$E = -e^{-\Sigma t} \int_0^z z' dz' - \int_0^z \tau dz' - \int_0^z \tau' dz' - \int_0^z \tau'' dz' - \dots$ which is the optical thickness seen by a neutron flying in the direction characterized by μ .

As z' (or τ) approaches zero, namely, as we refine the spatial grid, the above error is expanded near $\tau = 0$ as follows, $E = - + O(\tau^5) = O(\tau^2)$.

Therefore, the error introduced by flat source approximation is second order with respect to the mesh size.

3. Quadratic Component

Therefore, If the source is quadratic in space, the flat source approximation will converge to the true solution to third order, which is shown below.

Assuming $q(z') = z'^2, 0 < z' < z$, the error from Equation (20) can be evaluated, $E = -e^{-\Sigma t} \int_0^z z'^2 dz' - \int_0^z \tau z'^2 dz' - \int_0^z \tau' z' dz' - \int_0^z \tau'' dz' - \dots$ As $\tau \rightarrow 0$, the error approaches zero with third order, $\mu^2 E = - + O(\tau^6) = O(\tau^3)$.

However, since analytical solutions cannot be obtained directly from pure monomial sources, we instead manufactured corresponding monomial fluxes and generated the source term by substituting them into the left-hand side of Eq. (1).

Owing to the presence of the differential operator in Eq. (1), a quadratic neutron flux inevitably produces a source that contains both quadratic and linear components. The inclusion of this linear component leads to a degradation in the observed order of accuracy from third to second order, as the error associated with the linear term dominates the overall error convergence.

Moreover, with induction, it can be shown that the flat source approximation is generally second order accurate in space.

4. General Polynomial Component

For any source that can be expressed as $q(z') = z'^n$, the general form of polynomial sources, we can evaluate the error from Eq. (20) as follows:

$E(n) = -e^{-\Sigma t} \int_0^z z'^n dz' - \int_0^z \tau z'^n dz' - \int_0^z \tau' z'^{n-1} dz' - \int_0^z \tau'' z'^{n-2} dz' - \dots$ (28) $E(n+1) = - \int_0^z \tau z'^{n+1} dz' - \int_0^z \tau' z'^n dz' - \int_0^z \tau'' z'^{n-1} dz' - \dots$

source moment is defined as, $MMS(\mu) = \int_0^z z' q(z') dz' - zc q(z', \mu)$. The following source cases are the same as Sect. II A.

3. Quadratic Component

It is straightforward to demonstrate that the linear source approximation can represent a flat source without errors.

Since q_1 vanishes and q_0 exactly represents a constant source, the proof follows directly from Sect. II A 1.

2. Linear Component

Next, we demonstrate that the linear source approximation can exactly represent a linearly distributed source.

Assuming $q(z') = z'$, $0 < z' < z$ in q_0 and q_1 defined in Eq. (38) gives $\int_0^z z' q(z') dz' = \int_0^z z'^2 dz' = \frac{1}{2} z^2 = 1$. The approximating source distribution is exactly the same as the originally manufactured source distribution, as shown below $\tilde{q}(z') = q_0 + q_1$. From Eq. (37), the error $E(n=1)$ are given by $E(n=1) = -\int_0^z e^{-\Sigma t} e^{-\Sigma t} z q(z', \mu) dz' - \int_0^z e^{-\Sigma t} e^{-\Sigma t} z \tilde{q}(z', \mu) dz' = -\int_0^z z^2 dz' = -\frac{1}{2} z^2$. Last, if the source distribution is quadratic in space as $q(z') = z'^2$, $0 < z' < z$, we have $\int_0^z z' q(z') dz' = \int_0^z z'^3 dz' = \frac{1}{4} z^4$. Constructing the linear approximation with the zeroth and first source moments gives $\tilde{q}(z') = q_0 + q_1 z'$.

The error introduced via linear source (LS) approximation can be evaluated with Eq. (37). $E = -\int_0^z z^2 dz' - z \int_0^z z dz' = -\frac{1}{2} z^2 - \frac{1}{2} z^2 = -z^2$. The error approaches zero with fourth order as shown by Taylor expansion near $\tau = 0$. $E = -z^2 + O(\tau^4)$.

As mentioned in Sect. II A 2, we normally do not have a standalone quadratic source; rather, it usually comes with a linear component. Note that the linear component does not affect the accuracy of the linear source approximation, which can be explained by linear superposition. Since the linear source approximation represents the linear component exactly, the error only arises from the higher-order components.

To illustrate this, assume $q(z') = Cz' + z'^2$, $0 < z' < z$, where C is an arbitrary constant, then we have:

$\int_0^z z' q(z') dz' = \int_0^z (Cz'^2 + z'^3) dz' = \frac{C}{3} z^3 + \frac{1}{4} z^4$. Thus, the linear source approximation remains an exact representation of a linear source. $q(z') = (C + z) z'$. Therefore, the linear source approximating form is $\tilde{q}(z') = (C + z) z'$. Now the error associated with this approximation can be calculated using Eq. (37) as follows:

2. Testing Purely Absorbing Materials

To test the distributed source only, we chose purely absorbing materials, whose scattering cross section was set to zero.

Figures 4, 5, 6, 7 present the grid refinement results for four cases, each corresponding to a constant, linear, quadratic, or non-polynomial manufactured source.

- Figure 4 [Figure 4: see original paper] (Constant Source): The FS-MoC solution is exactly zero, as indicated by the absence of blue stars in the log-log scale plot. The LS-MoC solution, represented by orange stars, also exhibits near-zero errors for this case.
- Figure 5 [Figure 5: see original paper] (Linearly Distributed Source): The FS-MoC method demonstrates second-order accuracy, with the numerical results converging along the green line corresponding to the expected second-order convergence rate. The LS-MoC solution exhibits near-zero errors within machine precision, as it exactly represents the linear source distribution.
- Figure 6 [Figure 6: see original paper] (Quadratically Distributed Source): FS-MoC maintains second-order accuracy, while LS-MoC achieves fourth-order accuracy.
- Figure 7 [Figure 7: see original paper] (Non-Polynomial Source): Results indicate that FS-MoC and LS-MoC methods maintain second-order and fourth-order accuracy, respectively.

our previous research using the Method of Exact Solutions (MES) for the Ganapol case supports that our theoretical prediction can be generalized to 2D, which is documented in Sect. III B.

A. Verification Testing Using the Method of Manufactured Solutions The MMS is a widely used verification technique for assessing the correctness of numerical algorithms in scientific computing. Unlike traditional benchmark comparisons, MMS involves prescribing an exact analytical solution by introducing a manufactured source term into the governing equations. This approach enables the systematic testing of numerical methods by isolating discretization errors, ensuring consistency, and verifying the accuracy of computational models. MMS is particularly useful in complex multi-physics simulations, including neutron transport, fluid dynamics, and heat transfer, where analytical solutions are otherwise difficult to obtain.

1. Testing Suite

The 1D MoC code we developed has tested the formal order of accuracy for FS and LS approximations. Four test cases were devised, each based on an assumed flux shape and its corresponding manufactured source, both defined in the global coordinate system.

Test listings: Case 1: constant source distribution $\psi(x, \mu) = q$ MMS $(x, \mu) = 0(\Sigma_t - \Sigma_s)$ Case 2: linear source distribution $\psi(x, \mu) = q_0 + \mu q_1$ MMS $(x, \mu) = 0(\Sigma_t - \Sigma_s) + \mu q_1$ Case 3: quadratic source distribution $\psi(x, \mu) = q_0 + \mu q_1 + \mu^2 q_2$ MMS $(x, \mu) = 0(\Sigma_t - \Sigma_s) + 2\mu q_1$ Fig. 4. Order of accuracy with constant manufactured source (FS: exact, LS:

exact) Case 4: non-polynomial source distribution $\psi(x, \mu) = x + 1$ qMMS $(x, \mu) = x + 1 + (\Sigma_t - \Sigma_s) x + 1$ All experimental results align with analytical predictions, as summarized in Table 1, where the observed order of accuracy is presented alongside the formal order of accuracy in the format.

Fig. 5. Order of accuracy with linear manufactured source (FS: 2nd order, LS: exact) Fig. 7. Order of accuracy with non-polynomial manufactured source (FS: 2nd order, LS: 4th order) B. Verification Testing Using the Method of Exact Solutions The Method of Exact Solutions (MES) verifies numerical solutions by comparing them to known analytical expressions, typically sourced from the existing literature. These exact solutions provide precise values across all spatial and temporal points, enabling direct verification of numerical methods. If discrepancies remain within acceptable limits (e.g., round-off errors), the code is considered verified. Additionally, grid refinement studies can be conducted to analyze convergence behavior, either confirming theoretical expectations or establishing new benchmarks where none exist. Notably, the findings presented in this section originate from our previous work [20].

1. Ganapol benchmark

Benchmark Problem 3.4 from Ganapol’s analytical benchmark book [21] is a robust verification test case that can be implemented in MPACT [1] without special modifications to the code. This benchmark enables the verification of both our order-of-accuracy predictions and the accuracy of the MPACT code itself, as previously published in [15]. It also supports the broader code and solution verification activities for MPACT.

This case is presented again to confirm that the spatial convergence rate established in 1D extends to 2D problems. Below, we restate the problem configuration.

The Ganapol benchmark problem is an analytic, or “semi-analytic,” benchmark based on the exact solution of the singular integral equation that describes the single-group cylindrical transport problem. This solution methodology is a complex sequence of steps, which are described in detail in the book [21].

Fig. 6. Order of accuracy with quadratic manufactured source (FS: 2nd order, LS: 4th order) TABLE 1. Observed and formal order of accuracy Approx.

FS Pr. FS Ob. exact LS Pr. exact LS Ob. * The arrow indicates the aforementioned order degradation.

Quad. 3rd \rightarrow 2nd* Const. exact exact exact exact Non-poly.

The angular errors inherent in the numerical results were isolated using an error removal technique developed in a previous study [22].

The benchmark considers a homogeneous right circular cylinder of infinite height (Fig. 8 [Figure 8: see original paper]), characterized by: its boundaries. On

the other hand, the addition of a bounding box transforms the 1D cylinder configuration into a 2D fuel-pin problem.

Fig. 8. Infinite homogeneous cylinder • Radius: $r = R$ (measured in mean free paths) • Physical Radius: $r/\Sigma t$ • Height: $h \rightarrow \infty$ • Total cross section: Σt • Scattering cross section: Σs • Fission cross section: Σf • Secondary neutrons per collision: c , where $c = (\Sigma s + \nu \Sigma f) / \Sigma t$, ν is average of fission neutrons per fission.

The benchmark results are provided for several cases: (a) Uniform isotropic source - the scalar flux $\phi(r)$ is tabulated for selected values of $c < 1$; (b) Critical rod - the critical radius is tabulated as a function of $c > 1$; (c) Critical rod - the scalar flux $\phi(r)$ is depicted for critical rods as a function of $c > 1$.

Table 2, sourced from Ganapol [21], provides the benchmark results for the critical rod problem, listing the critical rod radius as a function of c . The values are accurate to the last known significant digit (within eight decimal points).

This table also confirms agreement with previously published benchmarks (i.e. [23, 24]), with discrepancies highlighted in bold results.

2. MPACT results

For MPACT verification, critical rod problems (b) in Sect. III B 1 are chosen as benchmarks because they exercise both the 2D MoC solver and the eigenvalue solver.

Because MPACT was used for LWR lattices, special input processing in the code is required to model the isolated cylinder. To avoid this, the benchmark is adapted by modeling the cylinder as a fuel pin within a non-scattering square bounding box (Fig. 9 [Figure 9: see original paper]). On the one hand, this approximation ensures the incoming angular flux remains zero outside the rod, with scattering and fission sources contributing only within Fig. 9. The material of the cylinder TABLE 2. Critical rod radii in MPACT from Table 3 .4.3(a) [21] R [24] MPACT determines the eigenvalue k based on the critical rod radii listed in Table 2. Each case should yield $k = 1$ to high precision, verifying the accuracy of the transport solution. The radial mesh was refined by increasing the number of rings.

All cases were run with the following phase space discretization parameters:

Bounding box side length = 30 cm Ray spacing = 0.0005 cm Number of radial rings = [10,160] by increment of 10 Number of azimuthal slices = 32 Quadrature set = CHEBYSHEV GAUSS 32 24 Convergence criterion = 10^{-7} for both k and RMS error of Table 3 presents the eigenvalues computed by MPACT, all within a few pcm of criticality. This confirms strong agreement with analytical solutions, reinforcing the reliability of MPACT.

TABLE 3. MPACT's k_{eff} and error R (mfp) Error(pcm)

3. Mesh convergence analysis

A radial mesh refinement study was conducted using the $c = 1.01$ case. The convergence curve in Fig. 10 [Figure 10: see original paper] demonstrates that MPACT achieves second-order accuracy in the radial direction, which is consistent with the FS-MoC expectations.

IV. CONCLUSIONS A comprehensive analysis of the order of accuracy related to spatial discretization in the MoC for slab geometry has been conducted, focusing on the flat source (FS) and linear source (LS) approximation of the distributed source. The study develops an analytical approach that integrates the angular flux using an assumed source term, yielding explicit expressions for the error in cell-averaged flux from source approximations, demonstrating that FS achieves at least second-order accuracy, whereas LS is expected to achieve fourth-order accuracy. These theoretical predictions were verified through numerical tests using the method of manufactured solutions (MMS) using a test suite that included constant, linear, quadratic, and non-polynomial solutions. The method of exact solutions (MES), utilizing the Ganapol critical rod problems, was also implemented using MPACT. The numerical results further verify the theoretical order of accuracy for the FS approximation in 2D.

These findings provide a rigorous foundation for assessing spatial discretization errors in MoC-based neutron transport. Future work will extend this analysis to the convergence behavior related to approximating the scattering source, ultimately helping determine the overall order of accuracy for spatial discretization in MoC.

V. CONTRIBUTION All authors contributed to the study conception and design.

Material preparation, data collection and analysis were performed by Jipu Wang, Zhenwen Wei and Can Huang. The first draft of the manuscript was written by Jipu Wang, Zhenwen Wei and Can Huang, and all authors commented on previous versions of the manuscript. All authors read and approved the final manuscript.

Fig. 10. Convergence with respect to radial discretization [1] A. Graham, E. W. Larsen, B. Collins, B. M. Kochunas S. Stimpson, Mpact 4.4 theory manual, Tech. rep., Oak Ridge National Laboratory (ORNL), Oak Ridge, TN (United States) (2023) [2] W. Boyd, S. Shaner, L. Li, B. Forget K. Smith, The Open-MOC method of characteristics neutral particle transport code. *Annals of Nuclear Energy* 68, 43–52 (2014). <https://doi.org/10.1016/j.anucene.2013.12.012> [3] J. Chen, Z. Liu, C. Zhao, Q. He, T. Zu, L. Cao H. Wu, A new high-fidelity neutronics code NECP-X. *Annals of Nuclear Energy* 116, 417–428 (2018). <https://doi.org/10.1016/j.anucene.2018.02.049> [4] A. Marin-Laflamme, M. Smith, C. Lee, Proteus-MOC: A 3D deterministic solver incorporating 2D method of characteristics, in: *International Conference on Mathematics and*

Computational Methods Applied to Nuclear Science and Engineering (M&C 2013), Sun Valley, ID, 2013 (2013) [5] B. M. Kochunas, A Hybrid Parallel Algorithm for the 3-D Method of Characteristics Solution of the Boltzmann Transport Equation on High Performance Compute Clusters, Phd Thesis, University of Michigan, Ann Arbor (2013) [6] J. Askew, A characteristics formulation of the neutron transport equation in complicated geometries, Tech. Rep.AEEW-R-1108, United Kingdom Atomic Energy Authority (1972) [7] J. Halsall, Cactus, a characteristics solution to the neutron transport equations in complicated geometries, Tech.

Rep.AEEW-R-1291, UKAEA Atomic Energy Establishment (1980) [8] D. Knott, A. Baratta, KRAM, A lattice physics code for modeling the detailed depletion of gadolinia isotopes in BWR lattice designs, in: Transactions of the American Nuclear Society; (United States)62, 1990 (1990), iISSN: ISSN 0003-018X [9] R. M. Ferrer, J. D. Rhodes, A Linear Source Approximation Scheme for the Method of Characteristics.

Nuclear Science and Engineering 182, 151-165 (2016). <https://doi.org/10.13182/NSE15-6> [10] S. Choi, A. Fitzgerald, N. Herring B. Kochunas, Linear Source Approximation in MPACT for Efficient and Robust Multiphysics Whole-Core Simulations. Nuclear Science and Engineering 198, 914-944 (2024). <https://doi.org/10.1080/00295639.2023.2224234> [11] J. Wang, W. R. Martin, T.

J. Downar, B. Kochunas, N. C. Andrews, L. Gilkey, E. D. Walker, B. S.

Collins M. Pilch, Code verification and solution verification framework in pin-resolved neutron transport code mpact. Annals of Nuclear Energy 178, 109365 (2022). <https://doi.org/https://doi.org/10.1016/j.anucene.2022.109365> [12] <https://www.casl.gov/CASL> | The Consortium For Advance Simulation Of Light Water Reactors [13] V. Mousseau, N. Dinh, CASL Verification and Validation Plan, Tech. Rep.CASL-U-2016-1116-000 (2016). <https://doi.org/10.2172/1431322> [14] J. Wang, Application of the Method of Manufactured Solutions to Verify the Method of Characteristics for Reactor Analysis, Phd Thesis, University of Michigan, Ann Arbor (2019) [15] J. Wang, Order of Accuracy of Spatial Discretization of Method of Characteristics, in: M&C 2017 - International Conference on Mathematics & Computational Methods Applied to Nuclear Science & Engineering, Jeju, Korea, 2017 (2017) [16] W. Ge, P. Wen, Z. Li, Q. Luo, C. Zhao, J. Wang M. Yang, APPLICATION OF THE METHOD OF MANUFACTURED SOLUTIONS TO VERIFY A NUCLEAR REACTOR PHYSICS COMPUTATIONAL CODE USING THE METHOD OF CHARACTERISTICS, Proceedings of International Conference on Nuclear Engineering (ICONE)2023.30, 2023, 1702 (2023). <https://doi.org/10.1299/jsmeicone.2023.30.1702> [17] P. J. Roache, The Method of Manufactured Solutions for Code Verification, in: C. Beisbart, N. J. Saam (Eds.), Computer Simulation Validation: Fundamental Concepts, Methodological Frameworks, and Philosophical Perspectives, Springer International Publishing, Cham, 2019, 295-318 (2019). <https://doi.org/10.1007/978-3-319->

70766-212 [18] E. W. Larsen, W. F. Miller Jr, Convergence rates of spatial difference equations for the discrete-ordinates neutron transport equations in slab geometry. Nuclear Science and Engineering 73, 76-83 (1980) [19] E. W. Larsen, P. Nelson, Finite-difference approximations and superconvergence for the discrete-ordinate equations in slab geometry. SIAM Journal on Numerical Analysis 19, 334-348 (1982) [20] J. Wang, W. R. Martin, T.

J. Downar, B. Kochunas, N. C. Andrews, L. Gilkey, E. D. Walker, B. S.

Collins M. Pilch, Code Verification and Solution Verification framework in pin-resolved neutron transport code MPACT. Annals of Nuclear Energy 178, 109365 (2022). <https://doi.org/10.1016/j.anucene.2022.109365> [21] B. Ganapol, Analytical Benchmarks for Nuclear Engineering Applications: Case Studies in Neutron Transport Theory, Tech.

Rep. ISBN 978-92-64-99056-2 (2009) [22] J. Wang, W. Martin, B. Collins, Application of the method of manufactured solutions to the 1D SN equation, in: Physics of Reactors 2016, PHYSOR 2016: Unifying Theory and Experiments in the 21st Century3, Sun Valley, ID, United states, 2016, 1434 -1451 (2016) [23] R. Sanchez, Generalization of Asaoka method to linearly anisotropic scattering: benchmark data in cylindrical geometry. [Integral transform method, matrix elements], Technical Report CEA-N-1831, CEA (1975) [24] J. R. Thomas, J. D. Southers, C. E. Siewert, The Critical Problem for an Infinite Cylinder. Nuclear Science and Engineering 84, 79-82 (1983). <https://doi.org/10.13182/NSE83-A17715>

Note: Figure translations are in progress. See original paper for figures.

Source: ChinaXiv – Machine translation. Verify with original.